International Forum on Aeroelasticity and Structural Dynamics
IFASD 2017
25-28 June 2017, Como - Italy

RIGID&ELASTIC COUPLING STABILITY ANALYSIS OF HYPERSONIC VEHICLES

Yan Yihan[1], Xie Changchuan[1], He Jingwu[1], Jiang Chongwen[1]

[1] School of Aeronautics Science and Engineering
Beihang University
lullabyyh@126.com

Keywords: local Piston, hypersonic, flight dynamics, coupling model

Abstract: This paper presents a framework of rigid&elastic coupling stability analysis of the hypersonic vehicles with complex configurations. Local piston theory based on CFD methods is introduced into the flight dynamic analysis process to take 3D effect into consideration. The flight dynamic equations considering elasticity are established in the coordinates of mean axes. Through the eigenvalue analysis of the state space equations, the longitudinal stability is discussed. And the influence of structural stiffness is discussed as well.

1 INTRODUCTION

The new generation of hypersonic vehicles is a hotspot for the moment in the fields of aerospace research on account of its important strategic value and economic benefit. And due to the wide use of lightweight multifunctional materials in modern hypersonic vehicles, the structural mass coefficient becomes smaller and the flexibility grows larger, which results in the coupling problem between rigid model and elastic model becoming much more obvious. The traditional rigid flight dynamics theory could no more satisfy the need of research. Schmidt and Chavez firstly brought up with the longitudinal dynamic model based on X-30 considering the coupling of elasticity [2]. The recent researches are mainly focusing on the flight dynamic characteristics, modeling[3] and stability analysis considering the elasticity of hypersonic vehicles. But at present stage of research, the hypersonic vehicles are usually being simplified as equal-section Euler beam of uniform material while studying the elastic deformation. And the aerodynamic theory is mainly restricted to Newtonian impact theory, shock expansion wave theory and piston theory. In this way, it is difficult to deal with the complex 3D structures, and the engineering applicability is poor. A flight dynamic theory with wide applicability coupling rigid and elastic model is needed.

In this paper, an effective method to calculate the aerodynamic forces and analyze the stability of the given model considering the coupling of rigid and elastic DOF is established. Considering the 3D effect and the hypersonic characteristics of model, a CFD-based local piston theory[5] is used as the method to calculate unsteady aerodynamic forces. Based on the mean axes and energy theory, the Lagrange equations of motion of the hypersonic vehicles are derived by the Hamilton's principle. Then, by employing the mode superpositon method and the small-disturbance assumption, the small-disturbance equations of motion are derived. Finally, the state-space model is established for the flight stability analysis by combining the equations of small-disturbance and unsteady aerodynamic model. The stability of the given model is solved by eigenvalue analysis of the characteristic matrix. A certain model similar to SR-72 is studied in this paper. And the influence of structural stiffness is considered.

2 THEORIES

2.1 Local Piston Theory Combined with CFD Results

As an effective engineering calculation method of quasi-steady aerodynamic forces, piston theory is widely used in the fields of aeroelastic and aerothermoelastic analysis of hypersonic vehicles under certain conditions. In order to enlarge the application field of this classic method, which is limited by the airfoil shape, angel of attack and Ma number, local piston theory was proposed. For the perturbations[4] are small relative to the mean steady state, we could apply the classic piston theory to calculate the perturbations relative to the local flow field which is accomplished by solving the Euler equations. In this way, the limitations of piston theory are removed. To get the perturbations of each point of the aerosurface, we could calculate the downwash w caused by the deviation of the moving surface which includes the deformation and vibration of each point. Then the formulation of local piston theory can be written as

$$\Delta p(x,y,z) = p_m - p_L = \rho_L C^2{}_L \left[\frac{w_m}{C_L} + \frac{\gamma+1}{4}(\frac{w_m}{C_L})^2 + \frac{\gamma+1}{12}(\frac{w_m}{C_L})^3 + \cdots \right] \tag{1}$$

Where ρ_L is the local density, C_L is the local sound speed. And keep the first-order terms, the equations become

$$\Delta p(x,y,z) = \rho_L C_L w \tag{2}$$

To derive the downwash w of any point on the three dimension aerosurface, we introduce the local coordinate system. Make the arbitrary point O as the origin of the coordinate with the exterior normal ζ and the direction of V_L as ξ, the local coordinate $O\xi\eta\zeta$ is set up.

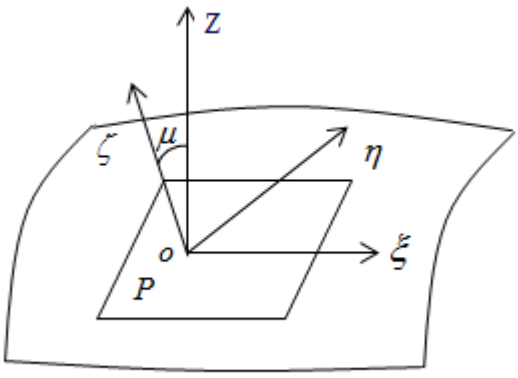

Figure 1: the local coordinate system

Assume the vibration of O is $\zeta(\xi,\eta,t)$,then the downwash could be expressed under this coordinate as

$$W_m = \frac{\partial}{\partial t}\zeta(\xi,\eta,t) + V_L \frac{\partial}{\partial \xi}\zeta(\xi,\eta,t) \tag{3}$$

Here we set up the structural coordinate system $Oxyz$, $Z(x,y,t)$ is the vibration of each point of the lifting surface. So, the downwash velocity in the structural coordinate is

$$W_m = \pm\mu\left(\frac{\partial Z}{\partial t} + V_L\left(\frac{\partial Z}{\partial x}\cos\alpha + \frac{\partial Z}{\partial y}\cos\beta\right)\right) = \pm\mu\left(\frac{\partial Z}{\partial t} + V_{Lx}\frac{\partial Z}{\partial x} + V_{Ly}\frac{\partial Z}{\partial y}\right) \tag{4}$$

$$\zeta = \pm\mu \cdot Z(x,y,t)$$

In which V_{Lx}, V_{Ly} is the local velocity in x and y direction. μ is the direction cosine of ζ and Z .And finally, the unsteady perturbation pressure of an arbitrary point on the three dimension lifting surface is

$$\Delta p = \pm\rho_L c_L \mu\left(\frac{\partial}{\partial t} + V_{Lx}\frac{\partial}{\partial x} + V_{Ly}\frac{\partial}{\partial y}\right)Z(x,y,t) \tag{5}$$

As mentioned above, to use the local piston theory, firstly the steady local flow field is needed. Several engineering methods of aerodynamic force calculating are widely used to solve the steady flow, such as the shock-expansion theory and Newtonian impact theory. However, these methods are not sufficiently accurate during the calculations, and cannot consider the three dimensions effect of a complex flow field. And if we use CFD (computational fluid dynamics) directly computing accurately unsteady loads, much time and resources are consumed, which apparently being not suitable for the engineering evaluation. So, the local piston theory combing with steady CFD results own the advantages of both methods by combing the accuracy of CFD and efficiency of engineering methods. The steady flowfield is computed by the CFD methods, then the unsteady aerodynamic could be solved by introducing the steady results into the local piston theory.

2.2 Surface Splines for Aerodynamic/structure Coupling

The surface spline[8] is used to transmit displacement and load between structure and aerodynamic models.

During the process of displacement interpolation, the relationship of the structure girds $\boldsymbol{X_S}$ and the displacements $\boldsymbol{U_s}$ could be described as

$$\mathbf{A}_S\mathbf{C} = \mathbf{W}_S \tag{6}$$

Where $\boldsymbol{A_s}$ is consistent of the information of the structure girds, $\boldsymbol{W_s}$ correspondingly contains the displacement information. And the coefficient matrix could be computed through the other two matrices based on the surface spline theory. Knowing $\boldsymbol{C}$, displacements of the aerodynamic grids could be written as

$$\mathbf{U}_A = \mathbf{A}_A\mathbf{A}_S^{-1}\mathbf{W}_S \tag{7}$$

Ultimately, the interpolation relationship between structure and aerodynamic models yields

$$\mathbf{U}_A = \mathbf{G}\mathbf{U}_S \tag{8}$$

where the spline matrix for displacement interpolation $\mathbf{G}$ is obtained by removing the first four columns of $\mathbf{A}_A\mathbf{A}_S^{-1}$.

While interpolating the forces, virtual work principle has to be satisfied:

$$\delta\mathbf{U}_A^{\mathrm{T}}\mathbf{F}_A = \delta\mathbf{U}_S^{\mathrm{T}}\mathbf{F}_S \tag{9}$$

where $\delta\mathbf{U}_A, \delta\mathbf{U}_S$ are arbitrary virtual displacement of aerodynamic grids and structure grids, respectively. Similarly, the relationship between load matrices of aerodynamic and structure models are

$$\mathbf{F}_S = \mathbf{G}^{\mathrm{T}}\mathbf{F}_A \tag{10}$$

2.3 Rigid/elastic Coupling Flight Dynamics

As demonstrated in the introduction, the aeroelastic effects of hypersonic vehicles are becoming much more significant and frequency separation between the rigid-body flight modes and elastic modes are much more reduced, which makes inertial coupling occurring between rigid body degrees of freedom and elastic degrees of freedom. The coupled equations of motion considering elasticity have a complex form, and makes it hard and unclear to analyze during the research of flight dynamics. To minimized the coupling problem, the mean axes[7] are used in the process of developing motion equations. The mean axes of which origin is the instantaneous mass center of the deformed vehicle are defined such that the relative linear and angular momenta[6], due to the elastic deformation, are zero at every instant, which means

$$\int_V \frac{\delta \boldsymbol{r}}{\delta t}\rho dV = \int_V \tilde{\boldsymbol{r}}\frac{\delta \boldsymbol{r}}{\delta t}\rho dV = 0 \tag{11}$$

In fact, by employing the assumption of small deformation and considering the location of mass center is invariant, the body-reference frame of a free-flight aircraft satisfies the mean axes constraints such that constitutes a mean-axis system, which means we could set the it as our analysis coordinate system. By using the Hamilton principle, the Lagrange's function can be obtained

$$\begin{aligned} T &= \frac{1}{2}M\boldsymbol{V}^{\mathrm{T}}\boldsymbol{V} + \frac{1}{2}\boldsymbol{\omega}^{\mathrm{T}}\boldsymbol{I}\boldsymbol{\omega} + \frac{1}{2}\dot{\boldsymbol{u}}^{\mathrm{T}}\boldsymbol{m}\dot{\boldsymbol{u}} \\ U &= \frac{1}{2}\boldsymbol{u}^{\mathrm{T}}\boldsymbol{k}\boldsymbol{u} \\ L &= T - U = \frac{1}{2}M\boldsymbol{V}^{\mathrm{T}}\boldsymbol{V} + \frac{1}{2}\boldsymbol{\omega}^{\mathrm{T}}\boldsymbol{I}\boldsymbol{\omega} + \frac{1}{2}\dot{\boldsymbol{u}}^{\mathrm{T}}\boldsymbol{m}\dot{\boldsymbol{u}} - \frac{1}{2}\boldsymbol{u}^{\mathrm{T}}\boldsymbol{k}\boldsymbol{u} \end{aligned} \tag{12}$$

And normal vibration modes are assumed to be available from a finite-element analysis

$$\boldsymbol{u} = \boldsymbol{\Phi}_e\boldsymbol{q}_e \tag{13}$$

Combine the above equations and use the Lagrange's Equations, finally after some simplifications the motion equations of rigid/elastic coupling are obtained

$$
\begin{aligned}
&M\dot{\boldsymbol{V}} - M\tilde{\boldsymbol{\omega}}^{T}\boldsymbol{V} = \boldsymbol{\Phi}_t^{\mathrm{T}}(\boldsymbol{f}_G + \boldsymbol{f}_A + \boldsymbol{f}_T)\\
&\boldsymbol{I}\dot{\boldsymbol{\omega}} + \tilde{\boldsymbol{\omega}}\boldsymbol{I}\boldsymbol{\omega} = \boldsymbol{\Phi}_r^{\mathrm{T}}(\boldsymbol{f}_G + \boldsymbol{f}_A + \boldsymbol{f}_T)\\
&\boldsymbol{M}_{ee}\ddot{\boldsymbol{q}}_e + \boldsymbol{B}_{ee}\dot{\boldsymbol{q}}_e + \boldsymbol{K}_{ee}\boldsymbol{q}_e = \boldsymbol{\Phi}_e^{\mathrm{T}}(\boldsymbol{f}_G + \boldsymbol{f}_A + \boldsymbol{f}_T) - \boldsymbol{M}_{ec}\ddot{\boldsymbol{\delta}}\\
&\dot{\boldsymbol{R}} = \boldsymbol{L}^{\mathrm{T}}\boldsymbol{V}\\
&\dot{\boldsymbol{\theta}} = \boldsymbol{D}^{-1}\boldsymbol{\omega}
\end{aligned}
\tag{14}
$$

Where $\boldsymbol{\Phi}_t^T, \boldsymbol{\Phi}_r^T, \boldsymbol{\Phi}_e^T$ are the rigid translation mode, rigid rotation mode and elastic mode; $\boldsymbol{M}_{ee}, \boldsymbol{B}_{ee}, \boldsymbol{K}_{ee}$ are the generalized mass matrix, damping matrix and stiffness matrix. $\boldsymbol{L}, \boldsymbol{D}$ are the transition matrices.

2.4 State Space Modeling and Stability Analysis

The dynamic equations obtained in section 2.3 are variable coefficient nonlinear differential equations, which makes it difficult to analyze the stability and other dynamic characteristics of the nonlinear system. By introducing the small-perturbation assumption, the variables can be expressed as the sum of the reference variable and the perturbation variable. While the longitudinal characteristics are more significant in the analysis of hypersonic vehicles, here we select the straight flight motion as the reference condition, which indicates $\dot{\boldsymbol{V}}_0 = \boldsymbol{\omega}_0 = \dot{\boldsymbol{\omega}}_0 = \dot{\boldsymbol{\theta}}_0 = 0$, $(\phi_0 \quad \theta_0 \quad \psi_0) = (0 \quad \pi \quad 0)$. If the ox axis of the mean axes frame $oxyz$ is defined parallel to the far field flow velocity vector, then we have $\boldsymbol{V}_0 = [u_0 \quad v_0 \quad w_0]^{\mathrm{T}} = [-V_\infty \quad 0 \quad 0]^{\mathrm{T}}$, which means $\alpha_0 = \beta_0 = 0$. Then the linearized small-perturbation equations are obtained

$$
\begin{aligned}
&M\Delta\dot{\boldsymbol{V}} - M\tilde{\boldsymbol{V}}_0\Delta\boldsymbol{\omega} = \boldsymbol{\Phi}_t^{\mathrm{T}}(\Delta\boldsymbol{f}_G + \Delta\boldsymbol{f}_A + \Delta\boldsymbol{f}_T)\\
&\boldsymbol{I}\Delta\dot{\boldsymbol{\omega}} = \boldsymbol{\Phi}_r^{\mathrm{T}}(\Delta\boldsymbol{f}_G + \Delta\boldsymbol{f}_A + \Delta\boldsymbol{f}_T)\\
&\boldsymbol{M}_{ee}\ddot{\boldsymbol{q}}_e + \boldsymbol{B}_{ee}\dot{\boldsymbol{q}}_e + \boldsymbol{K}_{ee}\boldsymbol{q}_e = \boldsymbol{\Phi}_e^{\mathrm{T}}(\Delta\boldsymbol{f}_G + \Delta\boldsymbol{f}_A + \Delta\boldsymbol{f}_T) - \boldsymbol{M}_{ec}\ddot{\boldsymbol{\delta}}\\
&\Delta\dot{\boldsymbol{R}} = \boldsymbol{L}_0\Delta\boldsymbol{V} - \boldsymbol{L}_0\boldsymbol{T}\Delta\boldsymbol{\theta}\\
&\Delta\dot{\boldsymbol{\theta}} = \boldsymbol{D}_0\Delta\boldsymbol{\omega}
\end{aligned}
\tag{15}
$$

In which, $\boldsymbol{L}_0, \boldsymbol{D}_0, \boldsymbol{T}$ are transition matrices

$$
\boldsymbol{L}_0 = \begin{bmatrix} -1 & 0 & 0 \\ 0 & 1 & 0 \\ 0 & 0 & -1 \end{bmatrix} \quad \boldsymbol{D}_0 = \begin{bmatrix} 1 & 0 & 0 \\ 0 & 1 & 0 \\ 0 & 0 & -1 \end{bmatrix} \quad \boldsymbol{T} = \begin{bmatrix} 0 & 0 & 0 \\ 0 & 0 & -V_\infty \\ 0 & -V_\infty & 0 \end{bmatrix} \tag{16}
$$

The right side of Eq.(15) are the generalized form of gravity, aerodynamic force and trust. In order to introduce the local piston theory to this analysis process, the method needs to be transformed to the generalized form. Substituting Eq.(13) to Eq.(5), the generalized form of aerodynamic forces can be written as

$$\begin{bmatrix} \boldsymbol{\Phi}_t^T \\ \boldsymbol{\Phi}_r^T \\ \boldsymbol{\Phi}_e^T \end{bmatrix} \Delta \boldsymbol{f}_A = \boldsymbol{B} \cdot \dot{\boldsymbol{q}}_S + \boldsymbol{C} \cdot \boldsymbol{q}_S$$

$$\begin{aligned} \boldsymbol{B} &= \boldsymbol{\Phi}^T \boldsymbol{S} \boldsymbol{A}_1 \boldsymbol{\Phi} \\ \boldsymbol{C} &= \boldsymbol{\Phi}^T \boldsymbol{S} \boldsymbol{A}_2 \frac{\partial \boldsymbol{\Phi}}{\partial \boldsymbol{x}} + \boldsymbol{\Phi}^T \boldsymbol{S} \boldsymbol{A}_3 \frac{\partial \boldsymbol{\Phi}}{\partial \boldsymbol{y}} \end{aligned} \tag{17}$$

Where $\boldsymbol{\Phi}^T = [\boldsymbol{\Phi}_t^T \ \boldsymbol{\Phi}_r^T \ \boldsymbol{\Phi}_e^T]$; $\boldsymbol{q}_S = [\boldsymbol{q}_R \quad \boldsymbol{q}_e]^{\mathrm{T}} = [\boldsymbol{q}_t \quad \boldsymbol{q}_r \quad \boldsymbol{q}_e]^{\mathrm{T}}$; $\boldsymbol{B}, \boldsymbol{C}$ are the aerodynamic coefficient matrices based on local piston theory; $\boldsymbol{S}$ is the area-weighted matrix, $\boldsymbol{A}_1, \boldsymbol{A}_2, \boldsymbol{A}_3$ are the local parameters computed by CFD. And $\boldsymbol{L}_{R0}, \boldsymbol{L}_{R1}$ are transition matrices.

$$\begin{aligned} \boldsymbol{q}_S &= \boldsymbol{L}_{R0} \boldsymbol{R}_S \\ \dot{\boldsymbol{q}}_S &= \boldsymbol{V}_S + \boldsymbol{L}_{R1} \boldsymbol{R}_S \\ \ddot{\boldsymbol{q}}_S &= \dot{\boldsymbol{V}}_S \end{aligned} \tag{18}$$

Substituting Eq.(17) to Eq.(15) , and write it into the form of matrix, we finally obtain the small-perturbation dynamic equation in the state space form for elastic aircraft

$$\dot{\boldsymbol{x}}_{ae} = \boldsymbol{A}_{ae} \boldsymbol{x}_{ae} + \boldsymbol{B}_{ae} \boldsymbol{\eta}$$

$$\begin{aligned} \boldsymbol{x}_{ae} &= \begin{bmatrix} \boldsymbol{R}_s \\ \boldsymbol{V}_s \end{bmatrix} \qquad \boldsymbol{A}_{ae} = \begin{bmatrix} \boldsymbol{L}_{s0} & \boldsymbol{L}_{s1} \\ \boldsymbol{M}_s^{-1}(\boldsymbol{B}\boldsymbol{L}_{R1} - \boldsymbol{K}_s + \boldsymbol{C}\boldsymbol{L}_{R0}) & \boldsymbol{M}_s^{-1}(\boldsymbol{B} - \boldsymbol{B}_s) \end{bmatrix} \\ \boldsymbol{h} &= \begin{bmatrix} 0 \\ \ddot{\delta} \end{bmatrix} \qquad \boldsymbol{B}_{ae} = \begin{bmatrix} \boldsymbol{0} \\ -\boldsymbol{M}_s^{-1}\boldsymbol{M}_c \end{bmatrix} \end{aligned} \tag{19}$$

By analyzing the eigenvalues of the state matrix $\boldsymbol{A}_{ae}$, the stability characteristics can be obtained. According to the stability criterion, if the real parts of all eigenvalues are negative, the system is stable; if the system contains the positive real parts of the eigenvalues, the system is unstable; and if the system has an imaginary eigenvalue and other eigenvalues have negative real parts, the system is critical stable.

3 NUMERICAL RESULTS

3.1 Structural Modeling

The model similar to SR-72 is constructed in ABAQUS as Figure 3. Considering the design characteristics of the new generation of hypersonic vehicles, such as near-space long endurance cruise with a high Mach number and the need of recycling, thin wall structures

with multi-functional lightweight material are mostly used in the model. The FEM(Finite Element Mode) is basically constructed by the triangular and quadrangular shell element. The triangular element is mainly used around the holes of the fuselage bulkhead. The details of design parameters are listed in Table 1.

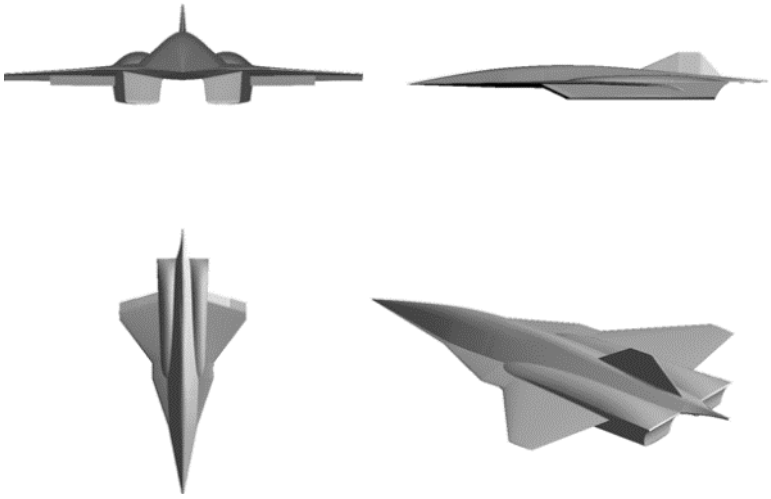

Figure 2: The Shape of the Model Similar to SR-72

	Parameters	Value
Geometry	Fuselage Length	30.00 m
	Fuselage Width	14.00 m
	Area	110.00 m^2
	Aileron Size	2.00 m*1.10 m
	Flap Size	2.70 m*1.20 m
Weight	Net Weight	1.126E+04 kg
Inertia	Ixx	2.36E+05 kg*m^2
	Iyy	2.98E+05 kg*m^2
	Izz	6.97E+04 kg*m^2

Table 1: Design Parameters of the Hypersonic Vehicle Model

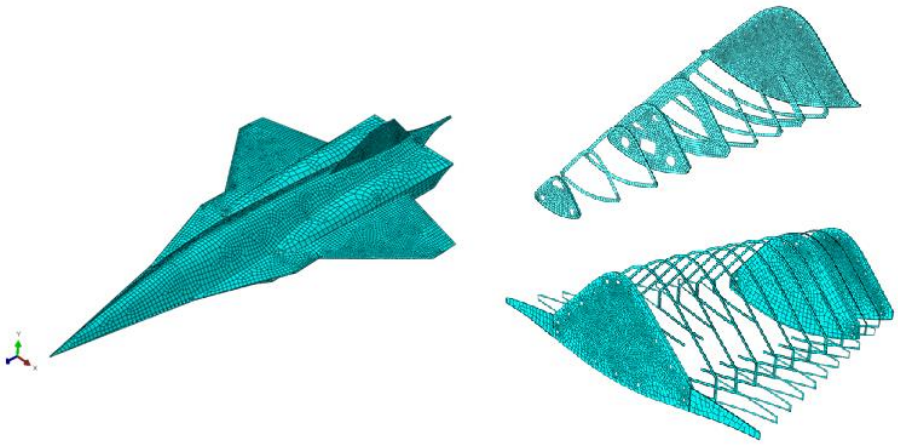

Figure 3 The Structural Finite Element Model

In the flight quality evaluation of hypersonic vehicles, we focus more on the short-period characteristics. If the short-period mode eigenvalues have a high frequency and large damping, the vehicle responses more quickly to the input of the control face. So, we pick three longitude motions of rigid body (moving forward, plunging, and pitching) as well as six symmetrical elastic vibration modes for the analysis of coupling flight dynamics. The modal frequencies and shapes are listed in Table 2.

Order	Frequency/Hz	Mode Name
Mode 1	0.00	Rigid translation
Mode 2	0.00	Rigid plunge
Mode 3	0.00	Rigid pitching
Mode 4	10.75	1st Wing Symmetric bending
Mode 5	23.12	1st Wing Symmetric torsion
Mode 6	35.63	2nd Wing Symmetric bending
Mode 7	41.80	2nd Wing Symmetric torsion
Mode 8	47.69	1st Fuselage Symmetric bending
Mode 9	59.87	3rd Wing Symmetric torsion

Table 2: Free-free Vibration Characteristics of Elastic Model

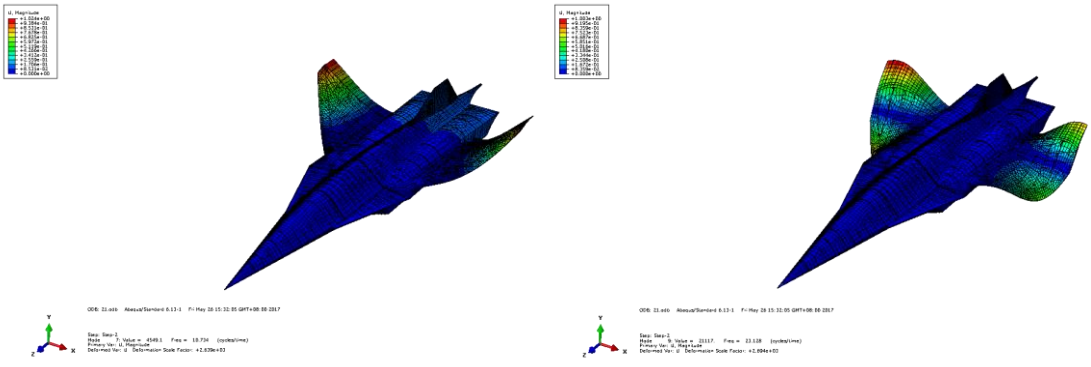

a. mode=4 **b. mode=5**

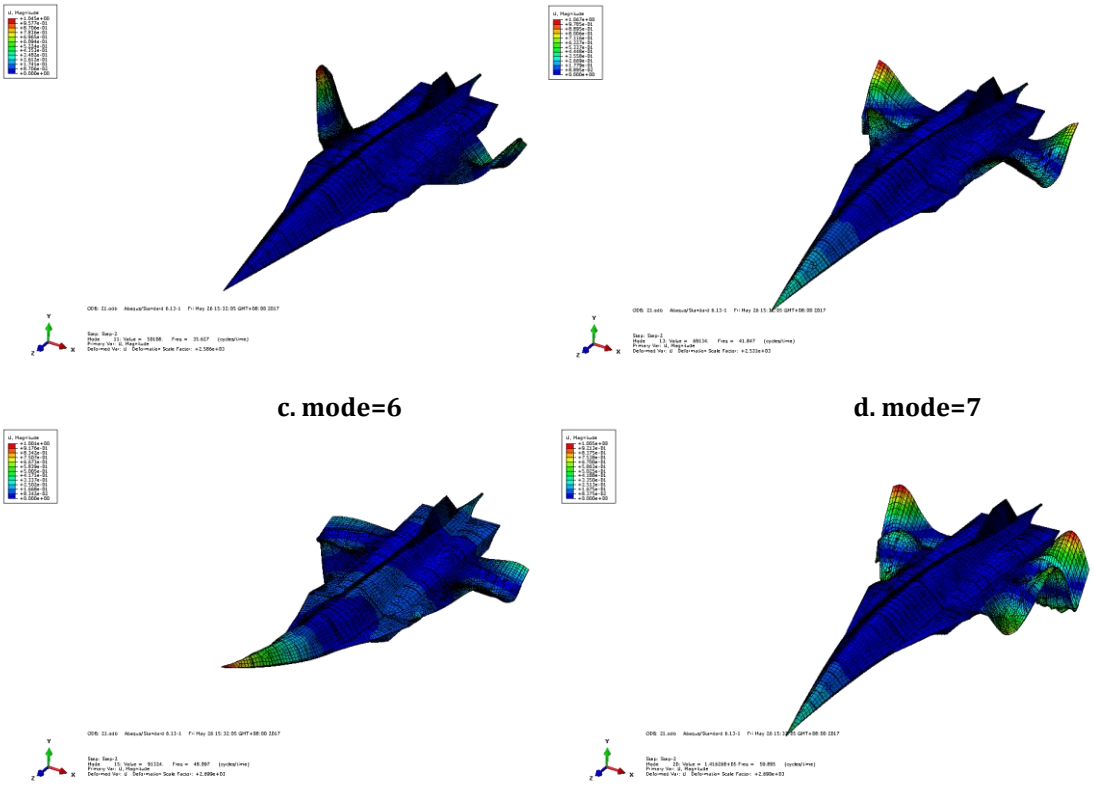

c. mode=6 **d. mode=7**

e. mode=8 **f. mode=9**

Figure 4: the first six symmetric modal shapes of elastic vibration

3.2 Aerodynamic Modeling

As demonstrated in section 2.1, steady flowfield is required in order to calculate the unsteady aerodynamics. In this article, the CFD methods are applied to get the local parameters of the aerodynamic configuration. Here we use Gridgen to generate the aerodynamic mesh (Figure 5) and accomplish the computation by solving inviscid Euler equations in Cart3D. The mesh quantity of the aerodynamic surface is about 220 thousand. Considering the typical cruise Ma number of such hypersonic vehicles, two typical conditions including, Ma=3.0 and Ma=6.0 are calculated. The contour of pressure and Ma are shown in Figure 6 and Figure 7. The variation of lift coefficient, drag coefficient and lift-drag ratio at Ma=3.0 as AOA grows is shown in Figure 8.

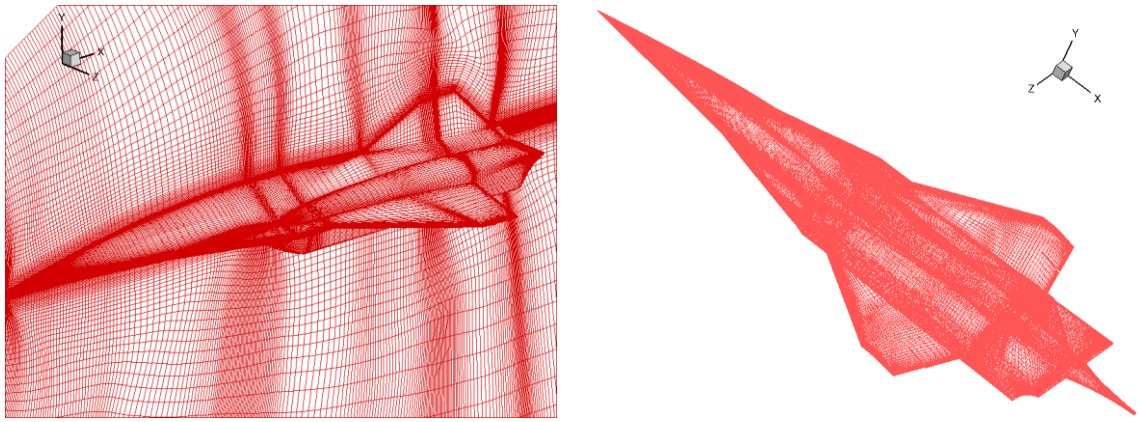

Figure 5: The Aerodynamic Mesh of The Model

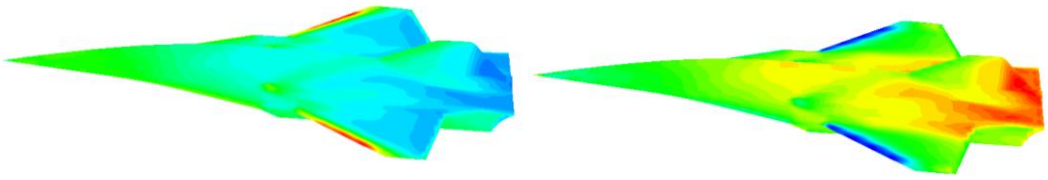

Figure 6 Pressure contour and Ma contour at Ma=3.0, AOA=1

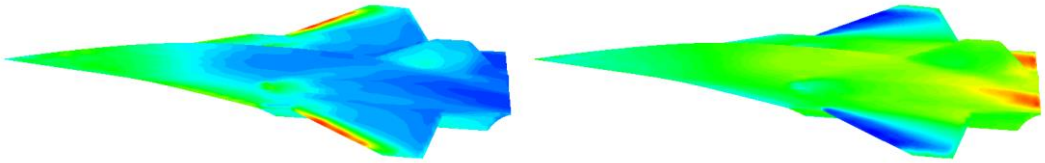

Figure 7 Pressure contour and Ma contour at Ma=6.0, AOA=0°

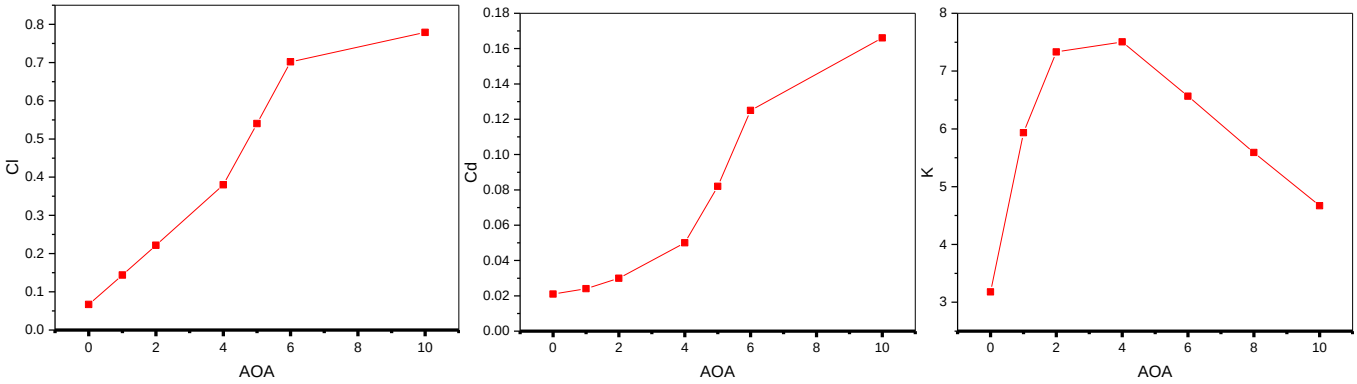

Figure 8 Variation of Cl, Cd, K at Ma=3.0 as AOA grows

3.3 Stability Analysis

In this article, the longitudinal flight dynamic characteristics of Ma=3.0 and Ma=6.0 are obtained by solving the eigenvalues of the state space equations which are assembled by the structural and aerodynamic modeling data. The eigenvalues of the pure rigid modes and rigid modes coupling elastic modes are listed in Table 3 and Table 4 to show the difference.

Mode	Eigenvalues	
	Rigid Model	Coupling Mode
Phugoid	-8.474E-03±1.479E-02i	-8.278±1.438E-02i
Shortperiod	-6.999±1.229i	-6.099±3.317i
1st Aeroelastic	—	-0.898±71.871i
2nd Aeroelastic	—	-2.294±147.88i

Table 3 Poles distribution comparison of rigid mode and coupling mode at Ma=3.0

Mode	Eigenvalues	
	Rigid Model	Coupling Mode
Phugoid	-4.419E-03±7.962E-03	-4.418E-03±7.960E-03
Shortperiod	-4.405±3.217i	-4.266±3.390i
1st Aeroelastic	—	-0.287±54.921i
2nd Aeroelastic	—	-1.097±117.11i

Table 4 Poles distribution comparison of rigid mode and coupling mode at Ma=6.0

By comparing the two tables, some conclusions can be drawn. As Ma number rises, both the real part and the imaginary part of the eigenvalues of phugoid decrease. For the real parts are both negative, the vehicle is stable in the phugoid mode. And the change of phugoid eigenvalues between the rigid model and coupling model is very little, which means in the freedom of plunge motion, no obvious coupling phenomenon occurs. Considering the phugoid mode possess a long period and the eigenvalues of the $\boldsymbol{A}_{ae}$ only present characteristic properties, detailed analyses are not discussed in this article. We focus more on the features of the shortperiod.

From the tables, we could found the damping and frequency of shortperiod both increase in the process of Ma number rising, which indicates the model studied in this paper equip with a better control character at a higher Ma number. For the frequency of shortperiod grows and becomes closer to the 1st aero elastic frequency which makes the rigid and elastic mode coupling. The motion properties of attack angel and pitching angular velocity which mainly reflect in the short period change due to the influence of the structural vibration. At Ma=3.0, the imaginary part of the shortperiod eigenvalue changes a lot while applying the coupling model. At Ma=6.0, the increasement is not that much, but both conditions have shown that the structural elasticity has a significant impact on the shortperiod mode.

To further illustrate the influence of the elastic mode, several conditions of different stiffness based on the original structural model at Ma=6.0 are computed. Open-loop zeros and poles of the short period mode and first four aeroelastic modes are drawn in Figure 9, and magnification of the short period mode is shown in Figure 10. It’s apparently that the frequency of the aeroelastic modes increases as the stiffness grows. And in Figure 10 we could found that the frequency of the short period becomes lower and the damping ratio grows larger while the stiffness grows.

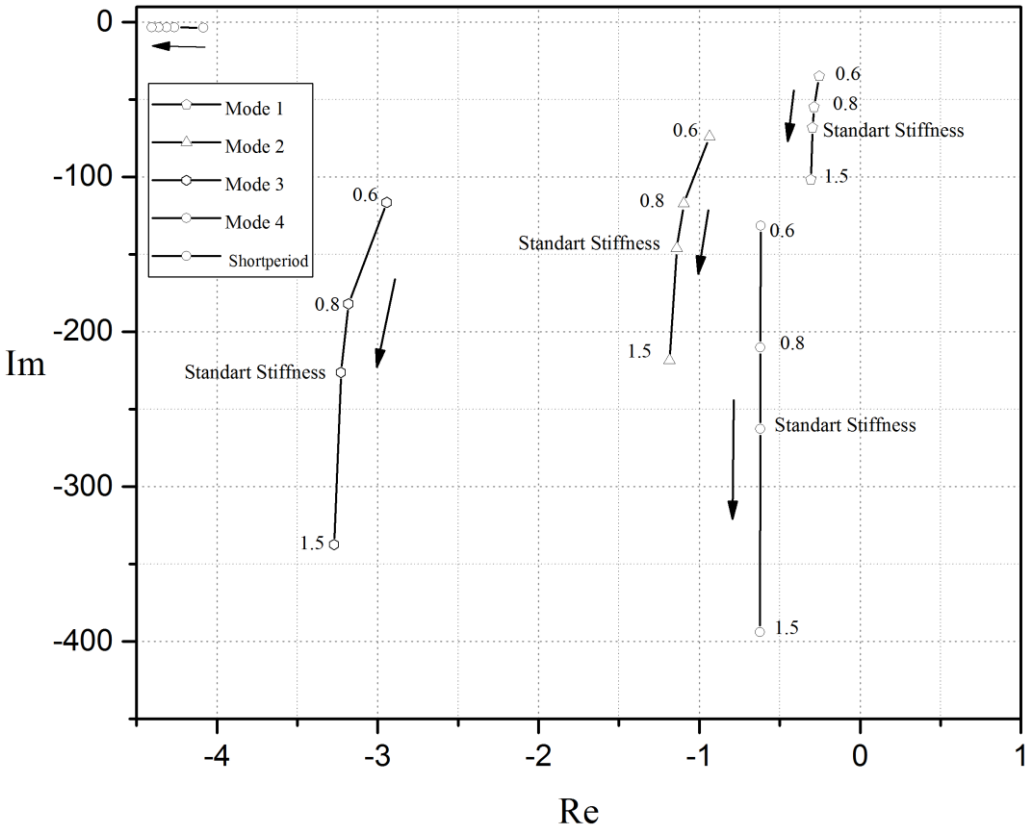

Figure 9 Eigenvalues of five modes changes with the variation of stiffness

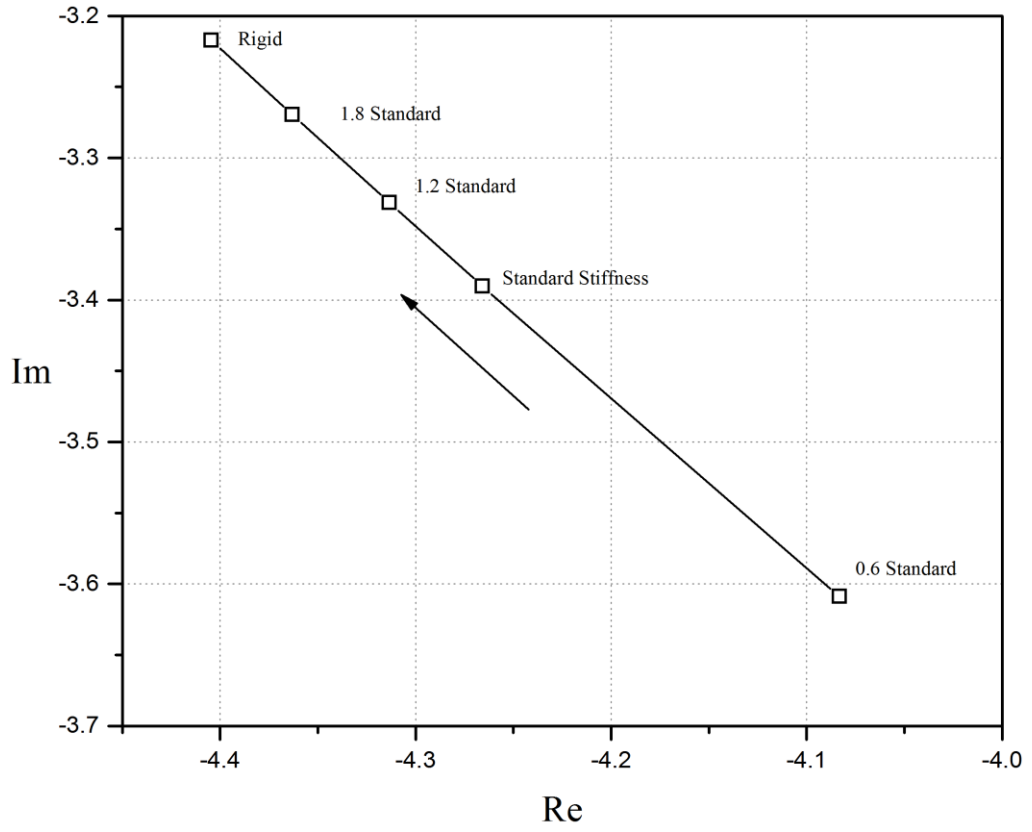

Figure 10 Eigenvalues of short period change with the variation of stiffness

4 CONCLUSION

In this paper, a framework of rigid&elastic coupling stability of hypersonic vehicles is established and a certain model similar to SR-72 is analyzed through the method. Local piston theory with CFD methods is applied to compute the unsteady aerodynamics of the complex aerodynamic configuration. Firstly, through the calculation of CFD, the body interference is taken into account and the precision of the steady flowfiled is guaranteed. And the unsteady flow field is solved by local piston theory using the CFD results to get the local parameters which are prepared for the AIC matrices. Based on traditional rigid flight dynamics, the mean axes are applied to decouple the rigid motion and elastic vibration. To analyze the longitudinal flight dynamic behaviors, three rigid modes and six elastic modes are picked to generalize the dynamic equations. And under the assumption of small-perturbation while the straight flight motion is selected as the reference condition the state space equations are established. Finally, by analyzing the eigenvalues of $\boldsymbol{A}_{ae}$, the longitudinal stability characteristics can be obtained. Through the research, the elastic modes have a significant influence on the short period eigenvalues. As the structural stiffness decreases, the frequency of the short period grows higher and the damping ratio becomes smaller. The present results are mainly focusing on confirming the efficiency of this analysis process. Further research about the flight dynamic properties of hypersonic vehicles will be studied in a more detailed and reliable model.

5 REFERENCE

[1] Yang C, Xu Y, Xie C. Review of Studies on Aeroelasticity of Hypersonic Vehicles[J]. Acta Aeronautica Et Astronautica Sinica, 2010.

[2] Chavez F R, Schmidt D K. Analytical aeropropulsive-aeroelastic hypersonic-vehicle model with dynamic analysis[J]. Journal of Guidance Control & Dynamics, 1994, 17(6):1308-1319.

[3] Bolender M A, Doman D B. Nonlinear Longitudinal Dynamical Model of an Air-Breathing Hypersonic Vehicle[J]. Journal of Spacecraft & Rockets, 2012, 44(2):374-387.

[4] Meijer M C, Dala L. Generalized Formulation and Review of Piston Theory for Airfoils[J]. Aiaa Journal, 2015, 54(1):1-11.

[5] Zhang Wei Wei, Shi Ai Min. Local piston theory combining steady CFD(in chinese)[J]. Journal of Northwestern Polytechnical University, 2004, 22(5)

[6] Bolender M A, Doman D B. Nonlinear Longitudinal Dynamical Model of an Air-Breathing Hypersonic Vehicle[J]. Journal of Spacecraft & Rockets, 2012, 44(2):374-387.

[7] Schmidt D. On the flight dynamics of aeroelastic vehicles[C].Astrodynamics Conference. 1986.

[8] Xie Changchuan, Yang Chao. Surface Splines Generalization and Large Deflection Interpolation, Journal of Aircraft, Vol. 44, N0. 3, May-June, 2007, 1024-1026

ACKNOWLEDGEMENT

This work was supported by the National-Key Reasearch and Development Program (2016YFB0200703).

COPYRIGHT STATEMENT